Journal of Advanced Research 32 (2021) 37–44

Contents lists available at ScienceDirect

Journal of Advanced Research

journal homepage: www.elsevier.com/locate/jare

Optimal bang-bang control for variable-order dengue virus; numerical studies ☆

N.H. Sweilam [a,b,*], S.M. AL-Mekhlafi [a,b], S.A. Shatta [c]

[a] Department of Mathematics, Faculty of Science, Cairo University, Giza, Egypt
[b] Academy of Scientific Research &Technology, 101 Al Kasr El Aini, Cairo, Egypt
[c] Department of Mathematics, Faculty of Science, Helwan University, Cairo, Egypt

HIGHLIGHTS

- A novel variable-order nonlinear model of dengue virus is analyzed as an optimal control problem.
- The bang-bang control is suggested to minimize the dose and duration of the intervention for model.
- Necessary conditions for the control problem are derived.
- Two numerical methods are constructed to solve the proposed optimal control problem.
- Comparative studies and numerical simulations are implemented.

GRAPHICAL ABSTRACT

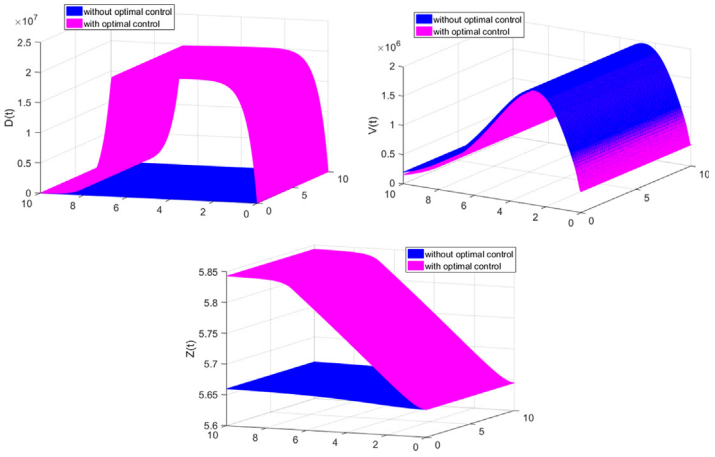

ARTICLE INFO

Article history:
Received 29 October 2020
Revised 14 February 2021
Accepted 22 March 2021
Available online 2 April 2021

Keywords:
Dengue virus
Variable order fractional model
Bang-bang control
Nonstandard generalized Euler method
Nonstandard generalized fourth order Runge-kutta method

ABSTRACT

Introduction: Dengue and Malaria are the most important mosquito-borne viral diseases affecting humans. Fever is transmitted between human hosts by infected female aedes mosquitoes. The modeling study of viral infections is very useful to show how the virus replicates in an infected individual and how the human antibody response acts to control that replication, which antibody playing a key role in controlling infection.
Objectives: Optimal control of a novel variable-order nonlinear model of dengue virus is studied in the present work. Bang-bang control is suggested to minimize the viral infection as well as quick clearance of the virus from the host. Necessary conditions for the control problem are given. The variable-order derivatives are given in the sense of Caputo. Moreover, the parameters of the proposed model are dependent on the same variable-order fractional power. Two numerical schemes are constructed for solving the optimality systems. Comparative studies and numerical simulations are implemented. The variable-order fractional derivative can be describe the effects of long variable memory of time dependent systems than the integer order and fractional order derivatives.
Methods: Both the nonstandard generalized fourth order Runge-Kutta and the nonstandard generalized Euler methods are presented.

☆ Peer review under responsibility of Cairo University.

* Corresponding author.
E-mail addresses: nsweilam@sci.cu.edu.eg (N.H. Sweilam), smdk100@gmail.com (S.M. AL-Mekhlafi), salmaasaad34@gmail.com (S.A. Shatta).

https://doi.org/10.1016/j.jare.2021.03.010

Results: We have successfully applied a kind of Pontryagin's maximum principle with bang-bang control and were able to reduce the viraemia level by adding the dose of DI particles. The nonstandard generalized fourth order Runge-Kutta method has the best results than nonstandard generalized Euler method. *Conclusion:* The combination of the variable-order fractional derivative and bang-bang control in the Dengue mathematical model improves the dynamics of the model. The nonstandard generalized Euler method and the nonstandard generalized fourth order Runge-Kutta method can be used to study the variable order fractional optimal control problem simply.

Introduction

Dengue and Malaria are the most important mosquito-borne viral diseases affecting humans. Fever is transmitted between human hosts by infected female aedes mosquitoes. The modeling study of viral infections is very useful to show how replication of virus in an infected cases and how acts the human antibody. The model presented in this paper confirmed the dynamics of defective interfering particles (DI) with virus. In [1] the authors give quantitative insight into the relationship between antibody levels and the efficiency of viral clearance. In [2], the authors keep the rate of infection and rate of antibody-mediated virus neutralisation constant for each serotype and included the immune cell-mediated antibody production, which is triggered by both the free virus and free defective particles. In [4], short fragments of dengue virus (DENV) RNA containing only key regulatory elements at the 3' and 5' ends of the genome were recovered from the sera of patients infected with any of the four DENV serotypes. Identical RNA fragments were detected in the supernatant from cultures of Aedes mosquito cells that were infected by the addition of sera from dengue patients, suggesting that the sub-genomic RNA might be transmitted between human and mosquito hosts in defective interfering (DI) viral particles. The authors in [5] conclude that DI particles may be important determinants of the course of acute, self-limiting viral infections and of porsistent, slowly progressing viral diseases. In addition, many host reactions may alter the production of DI particles and thus influence tho outcon1e of viral infections.

Recently, optimal control of diseases treatment has become popular in biology. In optimal control problems, it is sometimes the case that a control is restricted to be between a lower and an upper bound. If the optimal control switches from one extreme to the other (i.e., is strictly never in between the bounds), then that control is referred to be a bang-bang solution. Bang-bang controls frequently arise in minimum-time problems. Bang-bang solutions also arise when the Hamiltonian is linear in the control variable; application of Pontryagin's minimum or maximum principle will then lead to pushing the control to its upper or lower bound depending on the sign of the coefficient of u in the Hamiltonian. In order to find DI particles minimum dose, we used bang-bang control, that should be delivered to minimize viraemia duration and height, for more details on advantage of bang-bang control see ([6,7]).

Since integer order derivative is local in nature so it does not contain the complete memory and hence it does not describe the physical behavior of the model. To overcome this challenge, we use the fractional derivative. It is well known that fractional derivative is non-local in nature and due to this characteristic, it contains the whole memory and physical nature of the model. Fractional order models are used to determine the real world problems with a strategic solution. There are many mathematicians articles in this field, see for example ([21–24]).

On the other side, it is known that variable-order fractional derivative (VOFD) can be describe the effects of long variable memory of time dependent systems, but the integer order derivative can be used to characterize the short memory. Gómez-Aguilar et. al., in [8] studied the advantage of using variable order in the fractional ordinary differential equations (FODE) and proposed a new generalize numerical schemes for simulating variable-order fractional FODE operators with power-law, exponential-law and Mittag–Leffler kernel. Also, Chen et al., in [9] presented an interesting review on variable-order fractional differential equations. Also, Sweilam et al., introduced some numerical studies for variable-order fractional differential equations (VOFDEs), for more details see [10–15]. Recently, Sweilam and AL-Mekhlafi introduced some numerical studies for variable-order optimal control (VOC) models, for more details see [16–18].

The aim of this work is to extend the model of dengue virus which given in [2] to variable-order model with modified parameters. The bang-bang control is suggested to minimize the viral infection as well as quick clearance of the virus from the host. Necessary conditions for the control problem are given. The behavior of the proposed model will be studied by four numerical methods; the generalized Euler method (GEM), the generalized fourth-order Runge–Kutta method (GRK4M), the nonstandard generalized Euler method (NGEM) and the nonstandard generalized fourth-order Runge–Kutta method (NGRK4M). Comparative studies are given.

The rest of this paper is structured as follows: Some mathematical tools of VOFD are given in 'Notations and Preliminaries'. The proposed VOFD model with bang-bang control is introduced in 'Model Problem'. Numerical schemes for solving the optimality system are given in 'Numerical Methods for VOC Model'. Comparative studies and numerical simulations are presented in 'Numerical Simulations'. In 'Conclusions', the conclusions are introduced.

Notations and preliminaries

In this section, basic definitions of VOF calculus used in this paper are introduced [11]. Consider the following VOFDE:

$$ {}^{C}{}_{0}D_{t}^{\alpha(t)}y(t) = g(y(t),t), \quad 0 < \alpha(t) \leq 1, \quad 0 < t \leqslant T, \tag{1} $$

$y(0) = y_o$.

Caputo's variable-order fractional derivatives can be defined as follows:

Let $\Omega = \{[a,b], -\infty < a < b < +\infty, \alpha(t) \in \mathbb{C}\}, 0 < \alpha(t) < 1,$ the left–right hand side Caputo's derivatives of order $\alpha(t)$ for a function $y(t)$ are defined respectively:

$$ \begin{aligned} {}^{C}{}_{a}D_{t}^{\alpha(t)}y(t) &= \left[\int_a^t \frac{g^n(s)}{(t-s)^{1+\alpha(t)-n}}ds\right]\frac{1}{\Gamma(n-\alpha(t))}, \quad t > a, \\ {}^{C}{}_{t}D_{b}^{\alpha(t)}y(t) &= \left[\int_t^b \frac{g^n(s)}{(s-t)^{1+\alpha(t)-n}}ds\right]\frac{1}{\Gamma(n-\alpha(t))}, \quad t < b. \end{aligned} \tag{2} $$

For more details on VOFDE see ([11–18]).

Model problem

In the following, Dengue mathematical model which presented in [2] will be developed. This is extended to variable-order frac-

tional Dengue model with modified parameters, it is more general model than the model given in [2]. The competitive dynamics of the DI particles with virus is exhibited in the presence of the antibody response. Infected cells are categorized in two classes according to their stages of infection: early and late. The early infected cells (C_D *and* C_V) are available for super-infection, but the late cells (C_{V^*} *and* C_{VD}) are not because of the triggered interferon response and alteration in cell membrane receptor dynamics [2]. We use one control variable $u(t)$, the administration of excess DI particles to the model to reduce the viral infection as well as quick clearance of the virus from the host. Both the variables and parameters of proposed model are given in Tables 1 and 2 respectively. The general model is given as follows:

$$\begin{aligned}
&{}_0D_t^{\alpha(t)}C_U = r^{\alpha(t)}C_U(1-\tfrac{N}{K^{\alpha(t)}}) - k^{\alpha(t)}(V(t)+D(t))C_U(t) + \sigma^{\alpha(t)}C_D(t),\\
&{}_0D_t^{\alpha(t)}C_D = k^{\alpha(t)}(C_U D - C_D V) - \sigma^{\alpha(t)}C_D,\\
&{}_0D_t^{\alpha(t)}C_V = k^{\alpha(t)}(C_U V - C_V D) - (\pi_1^{\alpha(t)} + \mu^{\alpha(t)})C_V,\\
&{}_0D_t^{\alpha(t)}C_{V^*} = \pi_1^{\alpha(t)}C_V - \delta^{\alpha(t)}C_{V^*},\\
&{}_0D_t^{\alpha(t)}C_{VD} = k^{\alpha(t)}(C_V D + C_D V) + \mu^{\alpha(t)}C_V - \delta^{\alpha(t)}C_{VD},\\
&{}_0D_t^{\alpha(t)}V = \beta^{\alpha(t)}\pi_2^{\alpha(t)}C_{V^*} - \rho^{\alpha(t)}V - \varepsilon^{\alpha(t)}ZV,\\
&{}_0D_t^{\alpha(t)}D = \gamma^{\alpha(t)}\varphi^{\alpha(t)}C_{VD} - \rho^{\alpha(t)}D - \varepsilon^{\alpha(t)}ZD,\\
&{}_0D_t^{\alpha(t)}Z = \eta_1^{\alpha(t)}Z\tfrac{V}{\eta_2^{\alpha(t)}+V} + \eta_1^{\alpha(t)}Z\tfrac{D}{\eta_2^{\alpha(t)}+D}.
\end{aligned} \tag{3}$$

Let:

$$N(t) = C_U + C_D + C_V + C_{V^*} + C_{VD}.$$

Formulation of VOC bang-bang problem

In the following, we apply a kind of Pontryagin's maximum principle given in [3], to determine the necessary conditions for optimal control dengue virus model. Consider the following objective functional [2]:

$$J(u) = \min_{0\leqslant u\leqslant u_b}\int_{T_0}^{T_f}\left(\frac{1}{2}(a\,V^2(t) + b\,C_V^2(t)) + c\,u(t)\right)dt, \tag{4}$$

subjected to the constraint of the following system:

$$\begin{aligned}
&{}_0D_t^{\alpha(t)}C_U = r^{\alpha(t)}C_U(1-\tfrac{N}{K^{\alpha(t)}}) - k^{\alpha(t)}(V+D)C_U + \sigma^{\alpha(t)}C_D,\\
&{}_0D_t^{\alpha(t)}C_D = k^{\alpha(t)}(C_U D - C_D V) - \sigma^{\alpha(t)}C_D,\\
&{}_0D_t^{\alpha(t)}C_V = k^{\alpha(t)}(C_U V - C_V D) - (\pi_1^{\alpha(t)} + \mu^{\alpha(t)})C_V,\\
&{}_0D_t^{\alpha(t)}C_{V^*} = \pi_1^{\alpha(t)}C_V - \delta^{\alpha}C_{V^*},\\
&{}_0D_t^{\alpha(t)}C_{VD} = k^{\alpha(t)}(C_V D + C_D V) + \mu^{\alpha(t)}C_V - \delta^{\alpha(t)}C_{VD},\\
&{}_0D_t^{\alpha(t)}V = \beta^{\alpha(t)}\pi_2^{\alpha(t)}C_{V^*} - \rho^{\alpha(t)}V - \varepsilon^{\alpha(t)}ZV,\\
&{}_0D_t^{\alpha(t)}D = u(t) + \gamma^{\alpha(t)}\varphi^{\alpha(t)}C_{VD} - \rho^{\alpha(t)}D - \varepsilon^{\alpha(t)}ZD,\\
&{}_0D_t^{\alpha(t)}Z = \eta_1^{\alpha(t)}Z\tfrac{V}{\eta_2^{\alpha(t)}+V} + \eta_1^{\alpha(t)}Z\tfrac{D}{\eta_2^{\alpha(t)}+D},
\end{aligned} \tag{5}$$

Table 1
States of time for the model [2].

States	Description
C_U	The uninfected target cells.
C_D	The infected cells by defective interfering (DI) particles only.
C_V	The infected cells due to only by virus.
C_{V^*}	The virus infected.
C_{VD}	Cells infected by (DI) particles and virus.
V	The dynamics of standard virus i.e viraemia level.
D	The defective interfering (DI) particles.
Z	The antibody response, for more details see [2].

Table 2
All symbols in the system and their definition [2].

Symbols	Definitions	Values
Natural parameters (human hosting)		
$r^{\alpha(t)}$	Intrinsic rate of host cell proliferation.	$15.217^{\alpha(t)}$
$K^{\alpha(t)}$	Cellular carrying capacity of proliferation.	$(3.505e^{7})^{\alpha(t)}$
C_{U_0}	Uninfected level cells without illness.	$1e^{8}$
Serotype-specific parameters		
$\beta^{\alpha(t)}$	Number of V released per C_V cells after packaging.	$758.045^{\alpha(t)}$
$\varepsilon^{\alpha(t)}$	Antibody-mediated virus neutralisation.	$16.225^{\alpha(t)}$
$\gamma^{\alpha(t)}$	Number of D released per C_{VD}cells after packaging.	$38.259^{\alpha(t)}$
$k^{\alpha(t)}$	Rate of infection per virus.	$(2.45e^{-7})^{\alpha(t)}$
$\mu^{\alpha(t)}$	The rate mutation of V to D within host cells, turning C_V cells into C_{VD} cells.	$37.651^{\alpha(t)}$
$\rho^{\alpha(t)}$	Natural rate of clearance for D and V.	$9.562^{\alpha(t)}$
Parameters for patient-specific		
$\sigma^{\alpha(t)}$	Rate of loss of DI particles within host cells, turning C_U into C_D cells.	$(5.836e^{\pm 2})^{\alpha(t)}$
$\delta^{\alpha(t)}$	Death rate of infected cells.	$(2.426e^{\pm 2})^{\alpha(t)}$
$\eta_1^{\alpha(t)}$	Triggered immune rate by D or V, see [2].	$(1.607e^{\pm 2})^{\alpha(t)}$
$\eta_2^{\alpha(t)}$	Threshold parameter of the triggered immune cells proliferation.	$(2e^{10\pm 2})^{\alpha(t)}$
$\pi_1^{\alpha(t)}$	Rate of maturation of C_V cells into C_{V^*} cells	$(9.863e^{\pm 2})^{\alpha(t)}$
$\pi_2^{\alpha(t)}$	Rate at each C_{V^*} cells produces V cells.	$(68.503e^{\pm 2})^{\alpha(t)}$
$\varphi^{\alpha(t)}$	Rate at each C_{VD} cells produces D cells.	$(21.782e^{\pm 2})^{\alpha(t)}$
V_0	Viraemia level on the day 0 of illness.	$(3.6e^{5\pm 2})^{\alpha(t)}$
Z_0	Immune level response without illness.	$(5.645e^{-2\pm 2})^{\alpha(t)}$

where the constants a, b and $c$stand for the weighting constants, whereas T_0 and T_f are the initial and final time respectively. According to ([16,17]) the Hamiltonian is given as follows:

$$\begin{aligned}
&H(C_U, C_D, C_V, C_{V^*}, C_{VD}, V, D, Z, u, \lambda_i)\\
&= \frac{1}{2}(a\,V^2(t) + b\,C_V^2(t)) + c\,u(t) + \sum_{i=1}^{8}\lambda_i F_i,
\end{aligned} \tag{6}$$

where, λ_i are the adjoint variables or co-state variables and F_i is the right hand side of system (5) respectively, $i = 1,\ldots,8$.

The necessary conditions can be obtained by extension the conditions in [3] to variable order fractional as ([16–18]). These can be derived from (4) and (6):

$${}_0D_t^{\alpha(t)}\lambda_i(t) = -\frac{\partial H}{\partial g_i},\ g_i = \{V, D, Z, C_U, C_D, C_V, C_{V^*}, C_{VD}\}. \tag{7}$$

$$\begin{aligned}
&{}_0D_t^{\alpha(t)}C_U(t) = \tfrac{\partial H}{\partial \lambda_1},\ {}_0D_t^{\alpha(t)}C_D(t) = \tfrac{\partial H}{\partial \lambda_2},\\
&{}_0D_t^{\alpha(t)}C_V(t) = \tfrac{\partial H}{\partial \lambda_3},\ {}_0D_t^{\alpha(t)}C_{V^*}(t) = \tfrac{\partial H}{\partial \lambda_4},\\
&{}_0D_t^{\alpha(t)}C_{VD}(t) = \tfrac{\partial H}{\partial \lambda_5},\ {}_0D_t^{\alpha(t)}I_V(t) = \tfrac{\partial H}{\partial \lambda_6},\\
&{}_0D_t^{\alpha(t)}I_D(t) = \tfrac{\partial H}{\partial \lambda_7},\ {}_0D_t^{\alpha(t)}I_Z(t) = \tfrac{\partial H}{\partial \lambda_8},
\end{aligned} \tag{8}$$

$$\frac{\partial H}{\partial u} = \psi(t),$$

where $\psi(t)$ is a switching function, it can be negative or positive. A singular control will occurre when $\psi(t) = 0$. The particular time points, when the changes in sign of the switching function are defined as the switching points, where the duration between the switches are called the bang times [2].

Theorem 1. If u^* is the control variable with corresponding state $C_U^*, C_D^*, C_V^*, C_{V^*}^*, C_{VD}^*, V^*, D^*, Z^*$; then there exist adjoint variables λ_i^*, $i = 1,\ldots,8$, satisfies the following:

(i) adjoint equations:

$$
\begin{aligned}
{}^{C}_{t}D^{\alpha(t)}_{t_f}\lambda^*_1(t) &= -\lambda^*_1(r^{\alpha(t)}(1-\frac{N^*}{K^{\alpha(t)}}) - r^{\alpha(t)}\frac{C^*_U}{K^{\alpha(t)}} - k^{\alpha(t)}(V^*+D^*)) \\
&\quad - \lambda^*_2(k^{\alpha(t)}D^*) - \lambda^*_3 k^{\alpha(t)}V^*,
\end{aligned}
$$

$$
{}^{C}_{t}D^{\alpha(t)}_{t_f}\lambda^*_2(t) = \lambda^*_1(r^{\alpha(t)}\frac{C^*_U}{K^{\alpha(t)}} - \sigma^{\alpha(t)}) + \lambda^*_2(k^{\alpha(t)}V^* + \sigma^{\alpha(t)}) - \lambda^*_5 k^{\alpha(t)}V^*,
$$

$$
\begin{aligned}
{}^{C}_{t}D^{\alpha(t)}_{t_f}\lambda^*_3(t) &= -bC^*_V + \lambda^*_1(r^{\alpha(t)}\frac{C^*_U}{K^{\alpha(t)}} + \lambda^*_3(k^{\alpha(t)}D^* + \pi^{\alpha(t)}_1 + \mu^{\alpha(t)}) \\
&\quad - \lambda^*_4\pi^{\alpha(t)}_1 - \lambda^*_5(k^{\alpha(t)}D^* + \mu^{\alpha(t)}),
\end{aligned}
$$

$$
{}^{C}_{t}D^{\alpha(t)}_{t_f}\lambda^*_4(t) = \lambda^*_1(r^{\alpha(t)}\frac{C^*_U}{K^{\alpha(t)}} - \lambda^*_6(\beta^{\alpha(t)}\pi^{\alpha(t)}_2) + \delta^{\alpha(t)}\lambda^*_4,
$$

$$
{}^{C}_{t}D^{\alpha(t)}_{t_f}\lambda^*_5(t) = \lambda^*_1(r^{\alpha(t)}\frac{C^*_U}{K^{\alpha(t)}}) + \lambda^*_5\delta^{\alpha(t)} - \gamma^{\alpha(t)}\varphi^{\alpha(t)}\lambda^*_7,
$$

$$
{}^{C}_{t}D^{\alpha(t)}_{t_f}\lambda^*_6(t) = -aV^* + \lambda^*_1 k^{\alpha(t)}C^*_U + \lambda^*_2 k^{\alpha(t)}C^*_D - \lambda^*_3 k^{\alpha(t)}C^*_U - \lambda^*_5 k^{\alpha(t)}C^*_D + \lambda^*_6(\rho^{\alpha(t)} + \varepsilon^{\alpha(t)}Z^*) - \lambda^*_8\frac{\eta^{\alpha(t)}_1 Z^* \eta^{\alpha(t)}_2}{(\eta^{\alpha(t)}_2 + V^*)^2},
$$

$$
{}^{C}_{t}D^{\alpha(t)}_{t_f}\lambda^*_7(t) = \lambda^*_1 k^{\alpha(t)}C^*_U - \lambda^*_2 k^{\alpha(t)}C^*_U + \lambda^*_3 k^{\alpha(t)}C^*_V - \lambda^*_5 k^{\alpha(t)}C^*_V + \lambda^*_7(\rho^{\alpha(t)} + \varepsilon^{\alpha(t)}Z^*) - \lambda^*_8\frac{\eta^{\alpha(t)}_1\eta^{\alpha(t)}_2 Z^*}{(\eta^{\alpha(t)}_2 + D^*)^2},
$$

$$
{}^{C}_{t}D^{\alpha(t)}_{t_f}\lambda^*_8(t) = \lambda^*_6\varepsilon^{\alpha(t)}V^* + \lambda^*_7\varepsilon^{\alpha(t)}D^* - \lambda^*_8\eta^{\alpha(t)}_1(\frac{\eta^{\alpha(t)}_2 V^*}{\eta^{\alpha(t)}_2 + V^*} + \frac{\eta^{\alpha(t)}_2 D^*}{\eta^{\alpha(t)}_2 + D^*}), \tag{10}
$$

(ii) with transversality conditions:

$\lambda^*_i(T_f) = 0$, where $i = 1, 2, \ldots, 8$.

(ii) optimality condition:

$$
\begin{aligned}
&H(C^*_U, C^*_D, C^*_V, C^*_{V^*}, C^*_{VD}, V^*, D^*, Z^*, u, \lambda^*_i) = \\
&\min_{0\leqslant u\leqslant u_b} H(C^*_U, C^*_D, C^*_V, C^*_{V^*}, C^*_{VD}, V^*, D^*, Z^*, u^*, \lambda^*_i).
\end{aligned} \tag{11}
$$

The switching function

$$
\psi(t) = \frac{\partial H}{\partial u} = c + \lambda^*_7. \tag{12}
$$

So, u^* is bang-bang, and

$u^* = 0,\ \psi(t) < 0,$

$u^* = u_b,\ \psi(t) > 0.$

Proof. By (7), we get the system (10), where H^*:

$$
\begin{aligned}
H^* &= \tfrac{1}{2}(a\,V^{*2} + b\,C^{*2}_V) + c\,u^* + \lambda^*_1\,{}^{C}_{0}D^{\alpha(t)}_{t}C^*_U + \lambda^*_2\,{}^{C}_{0}D^{\alpha(t)}_{t}C^*_D + \lambda^*_3\,{}^{C}_{0}D^{\alpha(t)}_{t}C^*_V + \lambda^*_4\,{}^{C}_{0}D^{\alpha(t)}_{t}C^*_{V^*} \\
&\quad + \lambda^*_5\,{}^{C}_{0}D^{\alpha(t)}_{t}C^*_{VD} + \lambda^*_6\,{}^{C}_{0}D^{\alpha(t)}_{t}V^* + \lambda^*_7\,{}^{C}_{0}D^{\alpha(t)}_{t}D^* + \lambda^*_8\,{}^{C}_{0}D^{\alpha(t)}_{t}Z^*.
\end{aligned} \tag{13}
$$

The optimal control (12) can be obtained from the minimization condition (11). Then, we obtain the following state system:

$$
\begin{aligned}
&{}^{C}_{0}D^{\alpha(t)}_{t}C^*_U = r^{\alpha(t)}C^*_U(1-\tfrac{N^*}{K^{\alpha(t)}}) - k^{\alpha(t)}(V^*+D^*)C^*_U + \sigma^{\alpha(t)}C^*_D, \\
&{}^{C}_{0}D^{\alpha(t)}_{t}C^*_D = k^{\alpha(t)}(C^*_U D^* - C^*_D V^*) - \sigma^{\alpha(t)}C^*_D, \\
&{}^{C}_{0}D^{\alpha(t)}_{t}C^*_V = k^{\alpha(t)}(C^*_U V^* - C^*_V D^*) - (\pi^{\alpha(t)}_1 + \mu^{\alpha(t)})C^*_V, \\
&{}^{C}_{0}D^{\alpha(t)}_{t}C^*_{V^*} = \pi^{\alpha(t)}_1 C^*_V - \delta^{\alpha(t)}C^*_{V^*}, \\
&{}^{C}_{0}D^{\alpha(t)}_{t}C^*_{VD} = k^{\alpha(t)}(C^*_V D^* + C^*_D V^*) + \mu^{\alpha(t)}C^*_V - \delta^{\alpha(t)}C^*_{VD}, \\
&{}^{C}_{0}D^{\alpha(t)}_{t}V^* = \beta^{\alpha(t)}\pi^{\alpha(t)}_2 C^*_{V^*} - \rho^{\alpha(t)}V^* - \varepsilon^{\alpha(t)}Z^*V^*, \\
&{}^{C}_{0}D^{\alpha(t)}_{t}D^* = u^* + \gamma^{\alpha(t)}\varphi^{\alpha(t)}C^*_{VD} - \rho^{\alpha(t)}D^* - \varepsilon^{\alpha(t)}Z^*V^*, \\
&{}^{C}_{0}D^{\alpha(t)}_{t}Z^* = \eta^{\alpha(t)}_1 Z^*\tfrac{V^*}{\eta^{\alpha(t)}_2 + V^*} + \eta^{\alpha(t)}_1 Z^*\tfrac{D^*}{\eta^{\alpha(t)}_2 + D^*},
\end{aligned} \tag{14}
$$

where,

$N^* = C^*_U + C^*_D + C^*_V + C^*_{V^*} + C^*_{VD}.$

Numerical Methods for VOC Model

In this section, two nonstandard methods are constructed to simulate the optimality systems (10) and (14), for more details on NSFDM, see [20].

NGEM

The Euler method had been extended to study the variable-order fractional differential equations, for more details see [16] and the references cited therein. Consider a set of mesh points $\Im = \{t_o, t_1, \ldots, t_n\}$, such that $t_o = 0$, and $t_n = T$, where the step size $h = \frac{t_n}{n}$, $n = 1, 2, \ldots, N$.

The approximate solution of Eq. (1) using NGEM can be rewritten as follows [16]:

$$
y_{n+1} = y_n + \frac{\varphi(h)^{\alpha(t)}}{\Gamma(\alpha(t)+1)}g(y_n, t_n). \tag{15}
$$

Note that if $\alpha(t) = 1$, then the NGEM reduces to the classical nonstandard Euler's method. The stability analysis of the fractional NGEM is investigated in ([12,16]).

NGRK4M

In the following, we will constructed a novel method called NGRK4M for solving the VOFDEs numerically. Using GRK4M [19], to approximate the solution of the Eq. (1), where, $\Im = \{t_o, t_1, \ldots, t_n\}$: $t_o = 0$, and $t_n = T$, and $h = \frac{t_n}{n}$, $n = 1, 2, \ldots, N$ is the step size. By substitute $\varphi(h)$ instead of h in GRK4M, where $\varphi(h)$ is a continuous function in h, and satisfies the following conditions:

$\varphi(h) = h + O(h^2),\ 0 < \varphi < 1,\ \forall\, h > 0.$

Then NGRK4M general formula is given as follows:

$$
y_{n+1} = y_n + \frac{1}{6}(K_1 + 2K_2 + 2K_3 + K_4), \tag{16}
$$

Table 3
The reduction value of viraemia level $V(t)$ when weighting constants $a = b = c = 1$, upper bounded $u_b = 2 \times 10^9$ and $t \in [0, 10]$.

$\alpha(t)$	GEM $h = 0.001$	NGEM $\varphi(h) = 0.025(1 - e^{-h})$	GRK4M $h = 0.001$	NGRK4M $\varphi(h) = 0.025(1 - e^{-h})$
$\alpha(t) = 1$	16%	22.1%	16.4%	22%
$\alpha(t) = 1 - 0.001t$	22.4%	29.4%	42.9%	51.8%
$\alpha(t) = 1 - 0.003t$	38.4%	47.9%	77.6%	85.1%
$\alpha(t) = 0.98 - 0.001t$	38.5%	48%	77.7%	85.3%
$\alpha(t) = 0.96 - 0.001t$	48.3%	69%	93.6%	96.9%
$\alpha(t) = 1 - 0.05e^{-t}$	16.5%	22.15%	16.4%	22%
$\alpha(t) = cos(0.005t)$	17.1%	23%	20.13%	26.27%
$\alpha(t) = 1 - 0.002\,sin^2(t)$	16.8%	22.5%	17.9%	23.7%
$\alpha(t) = 1 - 0.1\,sin^2(t)$	34.1%	43.2%	71.3%	79.8%

$$K_1 = \kappa f(t_n, y_n),$$

$$K_2 = \kappa f(t_n + \frac{1}{2}\kappa, y_n + \frac{1}{2}K_1),$$

$$K_3 = \kappa f(t_n + \frac{1}{2}\kappa, y_n + \frac{1}{2}K_2),$$

$$K_4 = \kappa f(t_n + \kappa, y_n + K_3),$$

where $\kappa = \frac{\varphi(h)^{\alpha(t)}}{\Gamma(\alpha(t)+1)}$,

Stability of NGRK4M

In order to study the stability of NGRK4M. Consider for simplicity the test problem:

$$^{c}{}_0D_t^{\alpha(t)} y(t) = \upsilon\, y(t), \quad 0 < t \leqslant T, \quad 0 < \alpha(t) \leq 1, \quad \upsilon < 0, \tag{17}$$

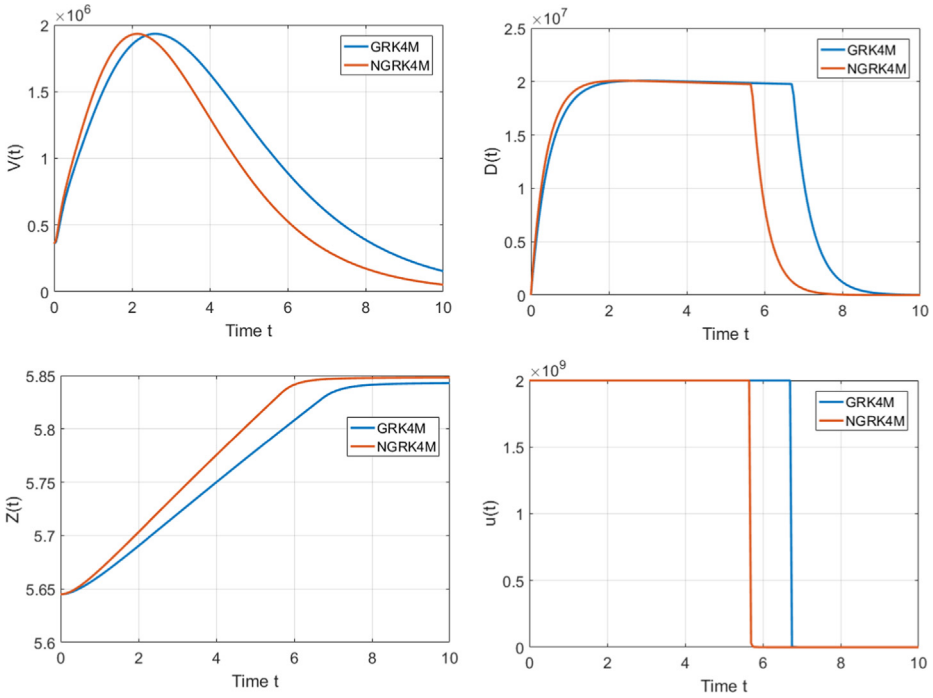

Fig. 1. Behavior of $V(t), D(t)$, and $u(t)$ when $a = b = c = 1$ and $\alpha(t) = 1 - 0.001t$ using GRK4M and NGRK4M.

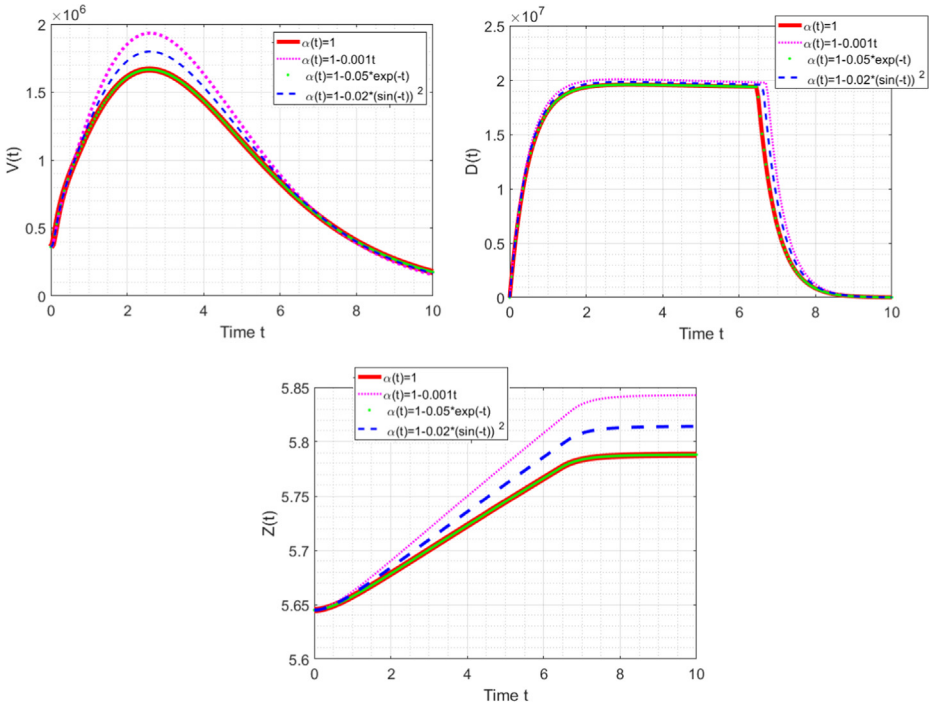

Fig. 2. Behavior of $V(t), D(t)$, and $Z(t)$ when $a = b = c = 1$ at different values of $\alpha(t)$ using NGRK4M.

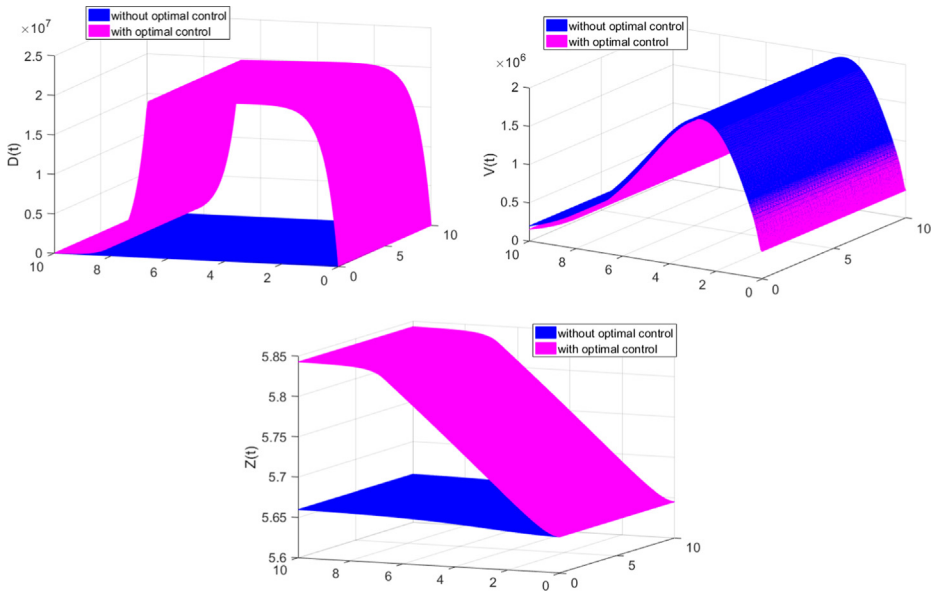

Fig. 3. Behavior of $V(t), D(t)$, and $Z(t)$ when $a = b = c = 1$ at $\alpha(t) = 1 - 0.001t$ with and without bang-bang optimal control.

$y(0) = y_o$, we can rewrite Eq. (17) using NGRK4M as follows:

$$y(t_{j+1}) = y(t_j) + \frac{1}{6}\frac{\varphi(h)^{\alpha(t)}\upsilon}{\Gamma(\alpha(t)+1)}y(t_j),\ j = 0, 1, \ldots, n-1. \tag{18}$$

The stability analysis of NGRK4M is similar to the NGEM method [12], when the terms are regrouped, the following equation is achieved:

$$y(t_{j+1}) = (1 + \frac{1}{6}\frac{\varphi(h)^{\alpha(t)}\upsilon}{\Gamma(\alpha(t)+1)})^{j} y_0,\ j = 0, 1, \ldots, n-1. \tag{19}$$

Then the stability condition [16] is given as follows:

$$-1 < (1 + \frac{1}{6}\frac{\varphi(h)^{\alpha(t)}\upsilon}{\Gamma(\alpha(t)+1)}) < 1,$$

$$0 < \varphi(h)^{\alpha(t)} < 12|\frac{\Gamma(\alpha(t)+1)}{\upsilon}|.$$

Numerical simulations

In the following, numerical simulations of the optimality systems (10) and (14) are presented. NGEM and NGRK4M are constructed to simulate these systems using the parameter values in Table 2. So we consider the initials states [2]: $C_U(0) = 10^8, C_D(0) = 0, C_V(0) = 100, C_{V^*}(0) = 0, C_{VD}(0) = 0, D(0) = 10^3, V_0 = 3.6 \times 10^5$, and $Z_0 = 5.645$. Table 3, shows the reduction values of viraemia level $V(t)$ when weighting constants $a = b = c = 1$, upper bounded $u_b = 2 \times 10^9$ and $t \in [0, 10]$ which is given as follows:

$$\text{Reduction} = \frac{V_{w.out} - V_w}{V_{w.out}} \times 100\%,$$

where, $V_{w.out}$ is viraemia level without bang-bang control treatment and V_w is viraemia level with bang-bang control treatment. Fig. 1, illustrates the behavior of the approximate solutions using GRK4M and NGRK4M. Fig. 2, shows the behavior of the state variables $V(t)$, $D(t)$ and $Z(t)$ with bang-bang control treatment and different value of $\alpha(t)$ using NGRK4M. Figs. 3 and 4, show the efficiency of the control treatment based on the densities of uninfected cells, viraemia level, DI particles and antibody particles with and without control. Fig. 3, shows that without treatments, the viraemia level is increasing up to some time. But after treatment of adding DI particles, the concentration of antibody particles are increasing up to some time and viraemia level is decreasing. Fig. 4, shows the effect of control treatment on viraemia and defective particles. Figs. 5 and 6, show the effect of DI high dose which reduce the viraemia and increase antibody particles in host body. Fig. 5, shows the behavior of the state $V(t), D(t), Z(t)$ and the optimal control $u(t)$ at different values of upper bounded when $\alpha(t) = 1 - 0.001t$ and $\varphi(h) = 0.025(1 - e^{-h})$ using NGRK4M. Fig. 6, shows the viraemia controlled treatment and particles defective at different values of upper bounded when $\alpha(t) = 1 - 0.001t$ and $\varphi(h) = 0.025(1 - e^{-h})$ using NGRK4M.

Conclusions

In the present work, optimal bang-bang control for a novel variable order fractional model of dengue virus is presented. The combination of variable order fractional derivative and optimal control in the model improves the dynamics and increases complexity of the model. We have successfully applied a kind of Pontryagin's

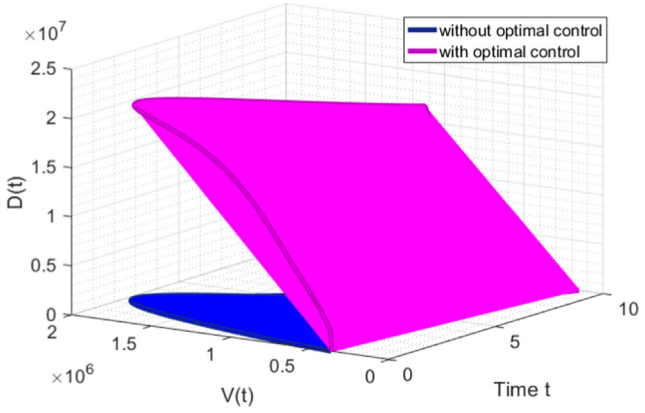

Fig. 4. Behavior of $V(t)$ and $D(t)$, when $a = b = c = 1$ and $\alpha(t) = 1 - 0.001t$ with and without bang-bang optimal control.

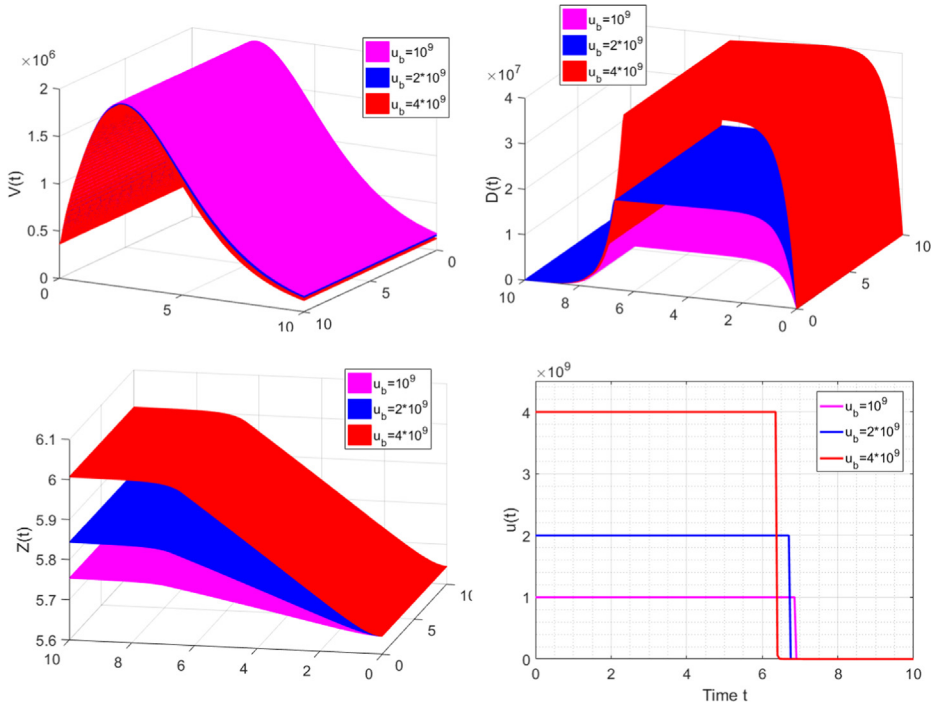

Fig. 5. Optimization of the dose treatment when $a = b = c = 1$ and $\alpha(t) = 1 - 0.001t$ at different values of upper bounded u_b.

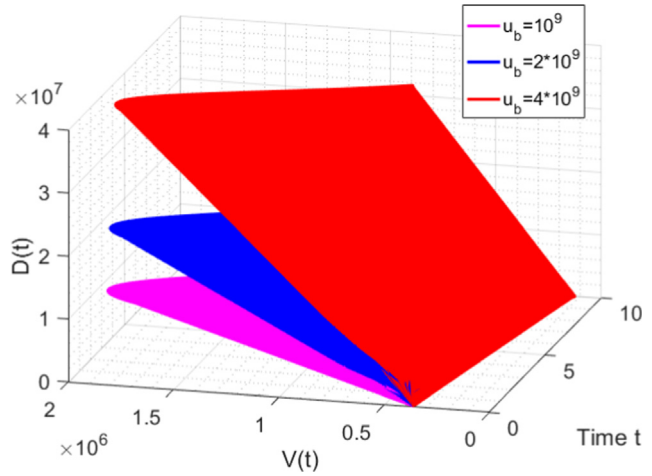

Fig. 6. Optimization of the dose treatment between $V(t)$ and $D(t)$ when $a = b = c = 1$ and $\alpha(t) = 1 - 0.001t$ at different values of upper bounded u_b.

maximum principle with bang-bang control to reduce the viraemia level by adding the dose of DI particles. NGEM and NGRK4M are used to study numerically the control problem. Mathematical analysis for NGEM and NGRK4M are introduced. Comparative studies are done and we can conclude from Table 3 that NGRK4M is the best than GEM, NGEM and GRK4M. Also from Fig. 2, we can conclude that the integer and fractional order models are special cases from the variable order model. Moreover, NGRK4M and NGEM can be used to study the variable order fractional optimal control problem simply.

Funding

This paper is supported by the Academy of Scientific Research and Technology (ASRT), Egypt, Grant 6454).

Compliance with Ethics Requirements

This article does not contain any studies with human or animal subjects.

Declaration of Competing Interest

The authors declare that they have no known competing financial interests or personal relationships that could have appeared to influence the work reported in this paper.

ASRT Acknowledgement

The authors would like to express their sincere thanks to the Academy of Scientific Research and Technology (ASRT), Egypt, Grant 6454), (ASRT) is the 2nd affiliation of this research.

References

[1] Clapham HE, Quyen TH, Kien DT, Dorigatti I, Simmons CP, Ferguson NM. Modelling virus and antibody dynamics during dengue virus infection suggests a role for antibody in virus clearance. PLoS Comput Biol 2015;12(5).
[2] Mapder T, Clifford S, Aaskov J, Burrage K. A population of bang-bang switches of defective interfering particles makes within-host dynamics of dengue virus controllable. PLoS Comput Biol 2019;15(11):1–24.
[3] Agrawal OP. A formulation and numerical scheme for fractional optimal control problems. IFAC Proc Vol 2006;39:68–72.
[4] Li D, Lott WB, Lowry K, Jones A, Thu HM, Aaskov J. Defective interfering viral particles in acute dengue infections. PloS One 2011;6(4).
[5] Huang AS, Baltimore D. Defective viral particles and viral disease processes. Nature 1970;226(5243):325–7.
[6] Lenhart SS, Workman JT. Optimal control applied to biological models, CRC Press; 2007.
[7] Ledzewicz U, Schättler H. Optimal bang-bang controls for a two-compartment model in cancer chemotherapy. J Optim Theory Appl 2002;114(3):609–37.
[8] Solís-Pérez JE, Gómez-Aguilar JF. Novel numerical method for solving variable-order fractional differential equations with power, exponential and Mittag-Leffler laws. Chaos, Solitons, and Fractals 2018;14:175–85.
[9] Sun H, Chang A, Zhang Y, Chen W. A review on variable-order fractional differential equations: mathematical foundations, physical models, and its applications. Fract Calc Appl Anal 2019;22(1):27–59.

[10] Sweilam NH, AL-Mekhlafi SM. Numerical study for multi-strain tuberculosis (TB) model of variable-order fractional derivatives. J Adv Res 2016;7 (2):271–83.
[11] Sweilam NH, Al-Mekhlafi SM, Albalawi AO. A novel variable-order fractional nonlinear Klein Gordon model: a numerical approach. Numer Methods Partial Differential Eq. 2019;35(5):1617–29.
[12] Sweilam NH, AL-Mekhlafi SM. Optimal control for a nonlinear mathematical model of tumor under immune suppression: a numerical approach. Optim Control Appl Meth 2018;39(5):1581–96. doi: https://doi.org/10.1002/oca.2427.
[13] Sweilam NH, AL-Mekhlafi SM, Shatta SA. On the awareness programs of the epidemic outbreaks fractional model. J Fract Calc Appl 2020;11(1):26–40. doi: https://doi.org/10.1002/oca.2427.
[14] Sweilam NH, AL-Mekhlafi SM, Shatta SA, Baleanu D. Numerical study for a novel variable-order multiple time delay awareness programs mathematical model. Appl Numer Math 2020;158: 212-235.
[15] Sweilam NH, AL-Mekhlafi SM, Shatta SA, Baleanu D. Numerical study for two types variable-order Burgers' equations with proportional delay. Appl Numer Math 2020;156: 364-376.
[16] Sweilam NH, AL-Mekhlafi SM, Alshomrani AS, Baleanu D. Comparative study for optimal control nonlinear variable-order fractional tumor model. Chaos, Solitons, and Fractals, 136; (2020).
[17] Sweilam NH, Mekhlafi SMAL, Albalawi AO, Tenreiro Machado JA. Optimal control of variable-order fractional model for delay cancer treatments. Appl Math Model 2020;89:1557–74.
[18] Sweilam NH, AL-Mekhlafi SM, Mohammed ZN, Baleanu D. Optimal control for variable order fractional HIV/AIDS and malaria mathematical models with multi-time delay. Alexandria Eng J, https://doi.org/10.1016/j.aej.2020.07.021; 2020.
[19] Milici C, Machado JT, Draganescu G. Application of the Euler and Runge-Kutta generalized methods for FDE and symbolic packages in the analysis of some fractional attractors. Int J Nonlinear Sci Numer Simul 2019;21(2).
[20] Mickens RE. Nonstandard finite difference models of differential equations. Singapore: World Scientific; 2005.
[21] Ameen I, Baleanu D, Ali HM. An efficient algorithm for solving the fractional optimal control of SIRV epidemic model with a combination of vaccination and treatment. Chaos Solitons Fractals 2002;137(109892). doi: https://doi.org/10.1002/mma.7022.
[22] Rashid S, Chu Y-M, Singh J, Kumar D. Unifying computational framework for novel estimates involving discrete fractional calculus approaches. Alexandria Eng J 2021;60(2):2677–85.
[23] Singh J, Ganbari B, Kumar D, Baleanu D. Analysis of fractional model of guava for biological pest control with memory effect. J Adv Res 2021. doi: https://doi.org/10.1016/j.jare.2020.12.004.
[24] Dubey VP, Dubey S, Kumar D, Singh J. A computational study of fractional model of atmospheric dynamics of carbon dioxide gas. Chaos, Solitons & Fractals 2021;142:110375. doi: https://doi.org/10.1016/j.chaos.2020.110375.